Implications of the Overlapping Degree Between Proximal Fibula and Tibia for Placing the Optimal Syndesmotic Screw: A Virtual Cadaveric Study

Gu-Hee Jung
Gyeongsang National University Hospital
Jun-Young Lee (leejy88@chosun.ac.kr)
Chosun university hospital https://orcid.org/0000-0002-9764-339X
Jae-Hwan Lim
Chosun University Hospital
Hyeon-Joon Lee
Chosun University Hospital
June-Yeon Lee
Chosun University Hospital

Research

Keywords: ankle, syndesmotic injury, screw fixation, three-dimensional modeling

Posted Date: January 25th, 2021

DOI: https://doi.org/10.21203/rs.3.rs-152552/v1

Version of Record: A version of this preprint was published at Indian Journal of Orthopaedics on June 15th, 2021. See the published version at https://doi.org/10.1007/s43465-021-00437-y.

Abstract

Background: To determine the optimal direction of the syndesmotic screw and introduce a consistent landmark for practical application by analyzing three-dimensional (3D) modeling and virtual implantation.

Methods: A total of 102 cadaveric lower legs (50 males and 55 females, average height of 160.6 ± 7.1cm) were used to reconstruct a 3D model by using the Mimics® software and the joint morphology was evaluated. Syndesmotic cylinders (Ø3.5 mm/Length 100 mm) were transversely placed in the proximal end of the incisura fibularis for simulating screw fixation. The tibial proximal cylinder, which was tangent to the posterior tibial condyles, was traced and the angle between the two cylinders was measured as the tibial torsion angle (TTA). After rotating the syndesmotic cylinder parallel to the ground, the overlapping degree between the proximal fibula and tibia were assessed as a radiologic indicator.

Results: Concerning tibial torsion, the TTA was an average of 36.7° (range, 17.2°–54.4°, SD 8.78) When the syndesmotic cylinder was rotated to be parallel to the ground, the proximal fibula had non- or linear overlap with the lateral border of the tibia, regardless of the joint morphology. In this nonoverlapping view, compared to the mortise view, the three criteria for normal fibular length could be better visualized.

Conclusion: The syndesmotic cylinder in the proximal end of the incisura fibularis could be consistently placed parallel to the ground by internally rotating the tibia until there was a non- or linear overlap between the proximal fibula and the tibia, regardless of the joint morphology.

Background

Syndesmotic injury/instability often occurs concurrently with ankle fractures and, until recently, has been treated solely with a transsyndesmotic screw. However, the dynamic suture-button technique has become more conventional owing to possible advantages compared to typical transsyndesmotic screws.[1] Regardless of the fixation options, the optimal trajectory of the guideline for positioning the definitive implant is the most important factor in preventing iatrogenic malreduction.[2, 3] Concerning the management of syndesmotic instability, first of all, surgeons intraoperatively verify the reduction adequacy by conventional radiography, including plain and fluoroscopic methods, without special equipment. Traditionally, the radiography of syndesmotic joints has been described in the anteroposterior (AP), lateral, and mortise views.[4] On the mortise view, the medial joint radiographic clear space between the talar dome and the distal tibia is within 2 mm. The leg must be rotated internally 15°–20°, thus aligning the intermalleolar line parallel to the detector and usually results in the 5th toe being directly in line with the center of the calcaneum.[5, 6]

As is well known, AP and mortise radiographs are inaccurate for determining the accuracy of syndesmotic reduction and compared to radiographs, postoperative computed tomography (CT) provides a better evaluation of the syndesmosis.[7] Often, the intraoperative fluoroscopic images demonstrate acceptable fibular position radiographically, but on the CT scan, the fibula is perched slightly anteriorly or posteriorly in the tibial incisura. Besides, considering the tibial torsion, which is an important anatomical parameter in clinical practice and displays variability among individuals[8], the rotational degree of the injured ankle cannot be determined and should be individualized by preoperative measurement of the noninjured contralateral leg. Thus, a recent study[9] reported the consistent landmark of the tibial tubercle as the TT view to assess the reduction adequacy of syndesmotic joint and make the optimal screw trajectory during the surgery. However, some orthopedic surgeons cited the potential limitations of clinical relevance due to the anatomic variation of tibial tubercles in the academic communication and congress of foot and ankle surgery.

Therefore, our next study sought to determine whether the usefulness of the tibial tubercle as an intraoperative landmark could be confirmed using other consistent and reliable structures. Based on the clinical experience of syndesmotic injury management, the authors have been using the overlapping degree between the proximal fibula and the lateral margin of the tibia as a consistent and reliable indicator to decide the adequacy of the leg's internal rotation. The principal objectives of this cadaveric study were: to verify the clinical relevance of the overlapping degree between the proximal fibula and the tibia, assess the morphology of the syndesmotic joint and implications of optimal fixation, and compare the practical usefulness between the tibial tubercle and the overlapping degree by analyzing three-dimensional (3D) models and virtual implantation of a syndesmotic screw in a 3D model.

Methods

Digital data of the human body were collected from the Korea Institute of Science and Technology Information (KISTI) and used by agreement. We used CT images of adult cadavers who underwent continuous 1.0 mm slice CT scans (Pronto, Hitachi, Japan) in the supine position. Based on a review of their records, cadavers with joint or tibiofibular bone problems were excluded. A total of 102 cadavers (49 males and 53 females) were enrolled. Their mean age at death was 52.4 years (range, 21–60 years; SD, 9.12) and their mean height was 160.4 cm (range, 146–176 cm; SD, 7.23). CT data in Digital Imaging and Communications in Medicine (DICOM) format were imported into Mimics® software (Materialise Interactive Medical Image Control System; Materialise, Antwerp, Belgium) to reconstruct 3D models, which included the tibia, fibula, and talus. After generating the 3D models, the CT scanning plane was reoriented to produce anatomical axial and coronal images parallel to the tibial plafond in the neutral rotation using the Mimics® software (Fig. 1).

An actual-size 3D cylinder model (Ø3.5 mm, length 100 mm) was created using 3D CAD software (SolidWorks 2019®, MA, USA) for simulating syndesmotic screw fixation in the distal tibiofibular joint. After obtaining 3D reconstructions of the bones and implant, virtual implantation of syndesmotic screws (syndesmotic cylinder) was performed via four synchronized windows composed of the axial plane, and coronal, sagiJol, and 3D biplanar images.[10–13] In the true coronal plane, a provisional line 1 mm in diameter at the proximal end of the incisura fibularis was placed for determining the height of the screw. In the axial plane, the provisional line was adjusted for bisecting the fibula and incisura fibularis and defined as the ideal syndesmotic cylinder trajectory.[9] Finally, after the syndesmotic cylinder was definitively placed along the provisional line, it was fine-tuned and verified several times by an experienced surgeon (first author, coauthors, and corresponding author). Next, for considering tibial torsion and its variability[8, 14], the tibial proximal cylinder (Ø3.5 mm/Length 150 mm), which was tangent to the posterior tibial condyles, was traced and the angle between the proximal cylinder and syndesmotic screw was measured for individual comparisons (Fig. 1).

Using the features of free 360° rotations with magnification in any plane, the morphology of the syndesmotic joint was assessed. The 3D models were rotated until the syndesmotic cylinder was parallel to the ground without any tilt, and this projection was defined as the syndesmotic AP projection. In the syndesmotic AP projection, the overlapping degree between the proximal fibula and the lateral border of the tibia was assessed for utilizing as a practical and consistent landmark. In addition, we evaluated various indicators, including the relationship between the adjacent bones, a nonirregular Shenton's line, and Weber's indices[3], and compared them with the conventional projection of the ankle mortise.

All measurements are presented as mean and range or binary variables, including the overlapping point, tibial torsion, and others. All statistical analyses were performed using the SPSS statistical software package for Windows version 25.0 (SPSS Inc., Chicago, IL, USA). Values of $p < 0.05$ were considered to be statistically significant.

Results

Concerning tibial torsion, the TTA was an average of 36.7° (range, 17.2°–54.4°, SD 8.78). The TTA in men (38.6° ± 8.66) and women (35.0° ± 8.60) in women was significantly different ($p = 0.038$). Regardless of individual variation in tibial torsion, the 3D biplanar images consistently showed that the proximal fibula was non- or linearly overlapping with the tibia in the syndesmotic AP projection of all models (Fig. 2 non-overlap). However, there was a clear space in the proximal tibiofibular joint in the true coronal scanning plane image. Concerning the tibial tubercle, it was directed superiorly and nearly vertical to the ground floor in the syndesmotic AP projection (Fig. 2).

Regarding the syndesmotic joint type, there were 44 cases of flat joints and 61 cases of crescent joints. The position of the distal fibula in the incisura was symmetric in 75 cases and asymmetric in 30 cases (29.4%). When comparing both, there were 20 cases of side differences (19.6%) in the distal fibula position (Fig. 3). Based on the side differences in the syndesmotic joint, there was no significance among continuous variables of the height of the cadaver, $p = 0.502$; the height of the incisura fibularis, $p = 0.497$; and the TTA, $p = 0.383$. The logistic regression analysis revealed that the joint type was $p = 0.498$ and symmetry was $p = 0.018$. When the Hosmer-Lemeshow goodness-of-fit test was performed with side difference as the dependent variable ($p = 0.613$), the joint symmetry was significantly different and the odds ratio was 3.50 (95%CI: 1.235–9.936, $p = 0.018$). Thus, joint symmetry had a significant impact on side difference; if the syndesmosis was symmetric in the incisura fibularis, the risk of a side difference was increased 3.5-fold.

The height of the incisura fibularis was an average of 26.6 mm (range, 21.1–32.7 mm, SD 2.51). According to sex, the height of the incisura fibularis was 26.2 mm ± 2.76 in men and 27.07 ± 2.21 in women and the difference was not statistically significant ($p = 0.067$). The height of the cadaver was 161.1c.m ± 7.56 in flat type joints and 160.2 cm ± 7.00 in crescent type joints, and there was no statistical significance ($p = 0.560$). The height of the incisura fibularis was 26.1 mm ± 2.46 in flat type joints and 27.04 ± 2.50 in crescent types and the difference was not statistically significant ($p = 0.053$). The degree of TTA was 36.8°± 7.52 in flat type joints and 36.6 ± 9.63 in crescent types, and the difference was not statistically significant ($p = 0.930$).

When the CT scanning plane was reformatted along the syndesmotic cylinder in the coronal plane, various indicators of a normal ankle joint were clearly identified in all models. Compared to the mortise view, the nonirregular Shenton's line of the ankle was better visualized as the medial spike of the distal fibula pointed exactly to the level of the joint space (Fig. 4). The coronal plane image of whole tibia and fibula demonstrated that the lateral border of the talus was always placed more medial than lateral to the distal tibia and the entire relationship between the fibula and the tibia in the incisura fibularis was easily identified (Fig. 4).

Discussion

Regarding the management of syndesmotic injury, it is widely known that there are two practical issues to diagnosing subtle instability and how to evaluate the intra- and postoperative reduction adequacy without special software and equipment. By this computational anatomy and simulation study, we identified the consistent radiologic indicators that might be used for assessing the intraoperative reduction adequacy according to variability in the tibial torsion and the depth of the incisura fibularis. As a result, this study found practical and interesting information that could be produced without special equipment. 1) The ideal screw trajectory was parallel to the ground if the leg was internally rotated such that the proximal fibular was non- or linearly overlapping with the tibia, regardless of individual variation in the tibial torsion and joint morphology. 2) Given the relatively high frequency of side differences (19.6%) and asymmetry (29.4%) of the syndesmotic joint, careful preoperative consideration of the opposite syndesmotic joint should be undertaken to guide the reduction adequacy. Thus, the intraoperative relationship, in which the lateral border of talus must always be just medial to the anterior tubercle in the syndesmotic AP projection, could help in the intraoperative assessment of reduction adequacy. 3) Eccentric movement of the fibula may not be occurred by the compressive force because our proposed trajectory and the position of the syndesmotic screw was the bisecting line of the fibula and incisura fibularis.

At the beginning of the study on the syndesmotic joint, the tibial tubercle (TT view) was used to determine the degree of internal rotation.[9] However, an inadequate screw trajectory was sometimes caused by insufficient internal rotation or excessive internal rotation (Fig. 5). Thus, first, the overlapping degree between the proximal fibula and the tibia was clinically applied to determine the syndesmotic screw trajectory, wherein our surgical experience proved useful and practical.[15] Henceforth, we performed the computational simulation study and demonstrated superiority over the tibial tubercle as a consistent landmark with less variation (Fig. 6). As mentioned in a previous study[9], through the syndesmotic AP projection, the screw trajectory and height, reduction adequacy, and relationship to the incisura fibularis could all be identified in real-time under standard fluoroscopic imaging and verified the positional change of the talus through the compressive force of the screw. Considering that subtle syndesmotic widening and fibular malreduction are notoriously difficult to measure by means of standard radiographic views[10, 16], our proposed technique might be of practical use without special or additional equipment.

This study also revealed interesting points by additionally measuring symmetry and the side differences in ankle syndesmosis, which had relatively high occurrences of 29.4% and 19.6%, respectively. Considering that the ankle joints with symmetry were 3.4 times more likely to have side differences, care should be taken when the opposite normal ankle joint is used to guide the reduction adequacy. The morphologic features of syndesmotic joint showed that 41.9% were flat joints and the incisura fibularis, with a mean 26.6 mm, was not significantly different according to joint type ($p = 0.053$) and sex ($p = 0.067$). Furthermore, its proximal end could be consistently utilized as a screw insertion point, regardless of variations. If the screw was inserted in the proximal end of the incisura fibularis through the syndesmotic AP projection, it is expected to have an ideal trajectory, which was the bisecting line of the fibula and the incisura fibularis.

However, our computational analysis had several fundamental limitations. All measurements were from normal ankle joints and thus, could have a rather descriptive character compared to the existing studies. Considering that accuracy and precision are the most important parameters for the evaluation of quantitative measurements for an area of known variability, there could be some errors in our results. In practical application of our overlapping method, there might be more radiation exposure of fluoroscopy compared with conventional or arthroscopic technique. If the tibia had deformity due to a disease or a previous fracture and combined fracture, there may be limitation. In case of high fibular fracture (maisonneuve fracture), the anatomical reduction and fixation should be given priority. In addition, proximal fibular overlapping may be difficult to identify in patients with multiple fractures due to position problems. Despite these limitations, our findings are valuable for understanding the anatomy of syndesmotic joints and the optimal trajectory of screws and will be helpful for assessing the reduction adequacy in intra- and postoperative images. The authors believe that the quantitative parameters of the morphological measurements were significant because they were based on scientific and reliable software analyzes. Regarding the report[17] that up to 80% of malreduction is present after syndesmotic fixation, a comparative clinical study through postoperative CT in the clinical practice would be required in the future.

Conclusion

Based on the computational analysis, the syndesmotic cylinder in the proximal end of the incisura fibularis could be consistently placed parallel to the ground by internally rotating the tibia until there was a non- or linear overlap between the proximal fibula and the tibia regardless of joint morphology.

List Of Abbreviations

3D Three-dimensional

CT Computed tomography

DICOM Digital Imaging and Communications in Medicine

KISTI Korea Institute of Science and Technology Information

PTFJ Proximal tibiofibular joint

TTA Tibial torsion angle

Declarations

- Ethics approval and consent to participate: This study was based on nationally recognized data and was exempted from IRB.
- Consent for publication: Not applicable
- Competing interests: All authors are listed above certify that they have NO affliations with or involvement in any arganization or entity with any financial interest, or non-financial interest in the subject matter or materials discussed in this manuscript.
- Funding: Not applicable
- Authors' contributions: Jun-Young LEE conceived the study and participated in its design and coordination and helped to draft the manuscript, and Gu-Hee Jung participated in the design of the study and wrote the manuscript, participated in the sequence alignment and drafted the manuscript. Jae-Hwan Lim performed the statistical analysis. Jun-Young LEE, Gu-Hee Jung, Jae-Hwan Lim fine-tuned and verified virtually placed syndesmotic cylinder along the provisional line. Hyeon-Joon Lee, June-Yeon Lee measured and collected data such as TTA, syndesmosis joint side difference, joint type, and height of fibular insisura.

References

1. Stiene A, Renner CE, Chen T, Liu J, Ebraheim NA. Distal tibiofibular syndesmosis dysfunction: a systematic literature review of dynamic versus static fixation over the last 10 years. J Foot Ankle Surg. 2019;58:320-7.
2. Westermann RW, Rungprai C, Goetz JE, Femino J, Amendola A, Phisitkul P. The effect of suture-button fixation on simulated syndesmotic malreduction: a cadaveric study. J Bone Joint Surg Am. 2014; 96:1732-8.

3. Futamura K, Baba T, Mogami A, Morohashi I, Kanda A, Obayashi O, Sato K, Ueda Y, Kurata Y, Tsuji H, Kaneko K. Malreduction of syndesmosis injury associated with malleolar ankle fracture can be avoided using Weber's three indexes in the mortise view. Injury. 2017;48:954-959.
4. Weber BG, Simpson LA. Corrective lengthening osteotomy of the fibula. Clin Orthop Relat Res.1985:61-7.
5. Croft S, Furey A, Stone C, Moores C, Wilson R. Radiographic evaluation of the ankle syndesmosis. Can J Surg. 2015;58:58-62.
6. Rammelt S, Zwipp H, Grass R. Injuries to the distal tibiofibular syndesmosis: An evidence-based approach to acute and chronic lesions. Foot Ankle Clin. 2008;13:611-33.
7. Loizou CL, Sudlow A, Collins R, Loveday D, Smith G. Radiological assessment of ankle syndesmotic reduction. Foot. 2017;32:39-43.
8. Gandhi S, Singla RK, Kullar JS, Agnihotri G, Mehta V, Suri RK, Rath G. Human tibial torsion–morphometric assessment and clinical relevance. Biomed J. 2014;37:10-3.
9. Lee JY, Lim JH, Jung GH. Radiological indicator of reduction adequacy during ankle syndesmosis surgery: A computational cadaveric study. Injury. 2018;49:1491-6.
10. Beumer A, Swierstra BA. The influence of ankle positioning on the radiography of the distal tibial tubercles. Surg Radiol Anat. 2003;25:446-50.
11. Ahn TK, Choi SM, Kim JY, Lee WC. Isolated syndesmosis diastasis: Computed tomography scan assessment with arthroscopic correlation. Arthroscopy. 2017;33:828-34.
12. Elgafy H, Semaan HB, Blessinger B, Wassef A, Ebraheim NA. Computed tomography of normal distal tibiofibular syndesmosis. Skeletal Radiol. 2010;39:559-564.
13. Ichiro Tonogai DH, Koichi Sairyo. Morphology of the Incisura Fibularis at the Distal Tibiofibular Syndesmosis in the Japanese Population. J Foot Ankle Surg. 2017;56:1147-50.
14. Hudson D. The rotational profile. A study of lower limb axial torsion, hip rotation, and the foot progression angle in healthy adults. Gait Posture. 2016;49:426-30.
15. Byun SE, Jung GH. Implications of three-dimensional modeling of tibia for intramedullary nail fixation: A virtual study on Asian cadaver tibia. Injury. 2020;51:505-9.
16. Taser F, Shafiq Q, Ebraheim N. Three-dimensional volume rendering of tibiofibular joint space and quantitative analysis of change in volume due to tibiofibular syndesmosis diastases. Skeletal Radiol. 2006,35:935-41.
17. Gardner MJ, Demetrakopoulos D, Briggs SM, Helfet DL, Lorich DG. Malreduction of the tibiofibular syndesmosis in ankle fractures. Foot Ankle Int. 2006;27:788-92.

Figures

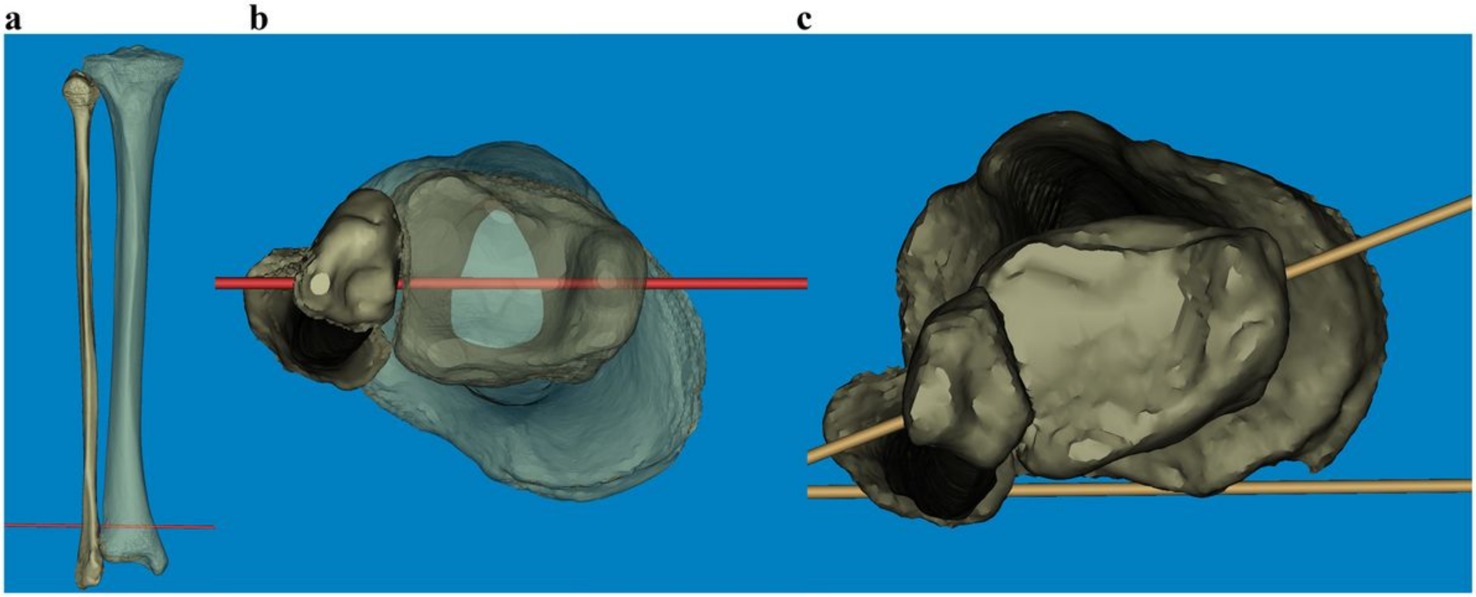

Figure 1

(A) After generating 3D models of the tibia and fibula, the syndesmotic cylinder was inserted in the proximal end of the incisura fibularis. (B) In the cephalad view of the 3D biplanar image, the trajectory of the cylinder was the bisecting line of the fibula and the incisura. (C) The tibial proximal cylinder, which was tangent to the posterior tibial condyles, was traced and the angle between the two cylinders was measured for individual comparison.

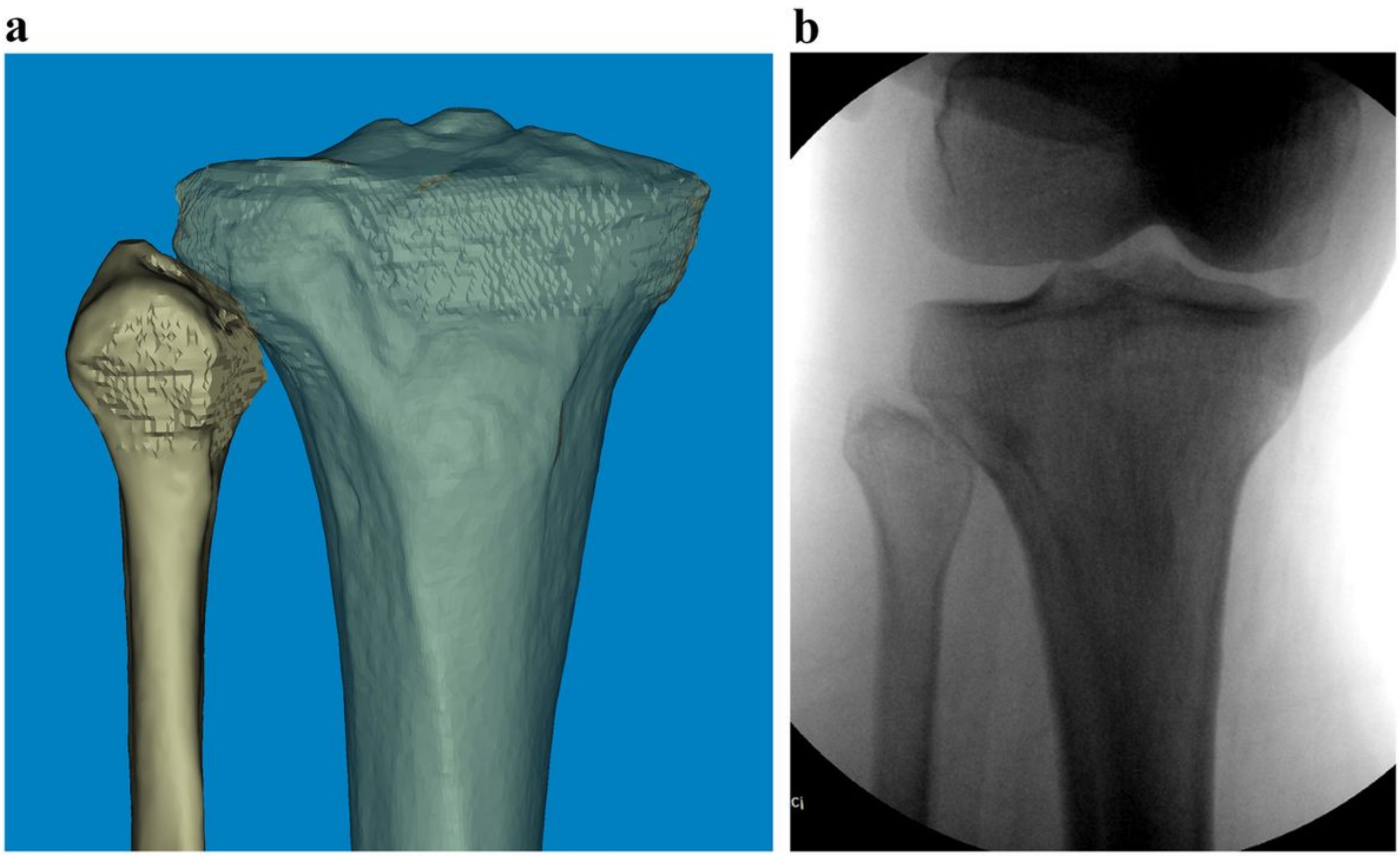

Figure 2

(A) The overlapping degree in the 3D biplanar images showed that the proximal fibular was non- or linearly overlapping with the tibia in the syndesmotic anteroposterior (AP) projection. (B) The fluoroscopic image showed a nonoverlapping degree in the syndesmotic AP projection.

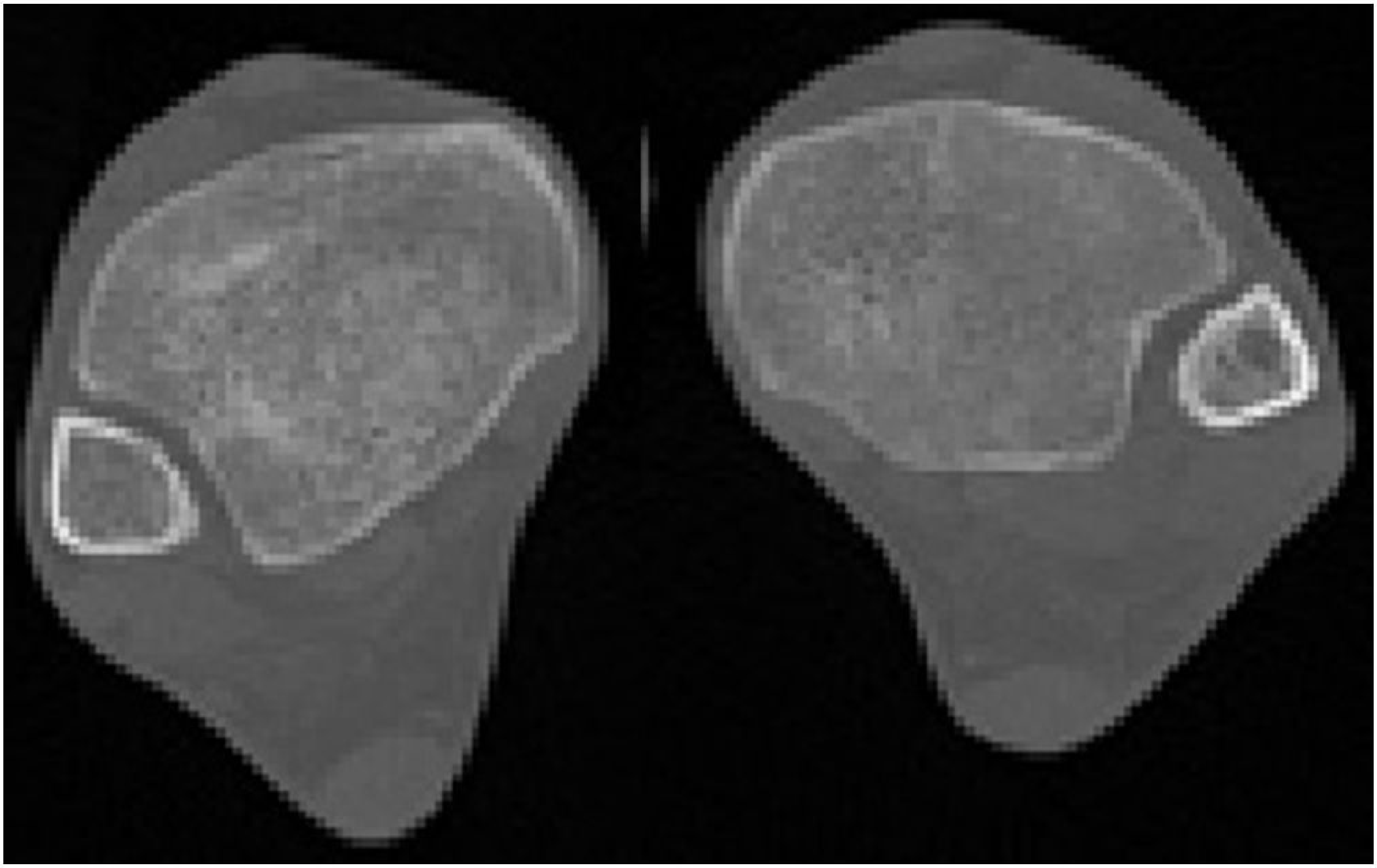

Figure 3

When comparing both legs, there was a side difference. The right leg was positioned symmetrically to the distal fibula in the incisura and the left leg was asymmetric.

Figure 4

When the computed tomography scanning plane was reformatted along the syndesmotic cylinder similar to the syndesmotic anteroposterior projection, the nonirregular Shenton’s line of the ankle was better visualized as the medial spike of the distal fibula pointed exactly to the level of the joint space.

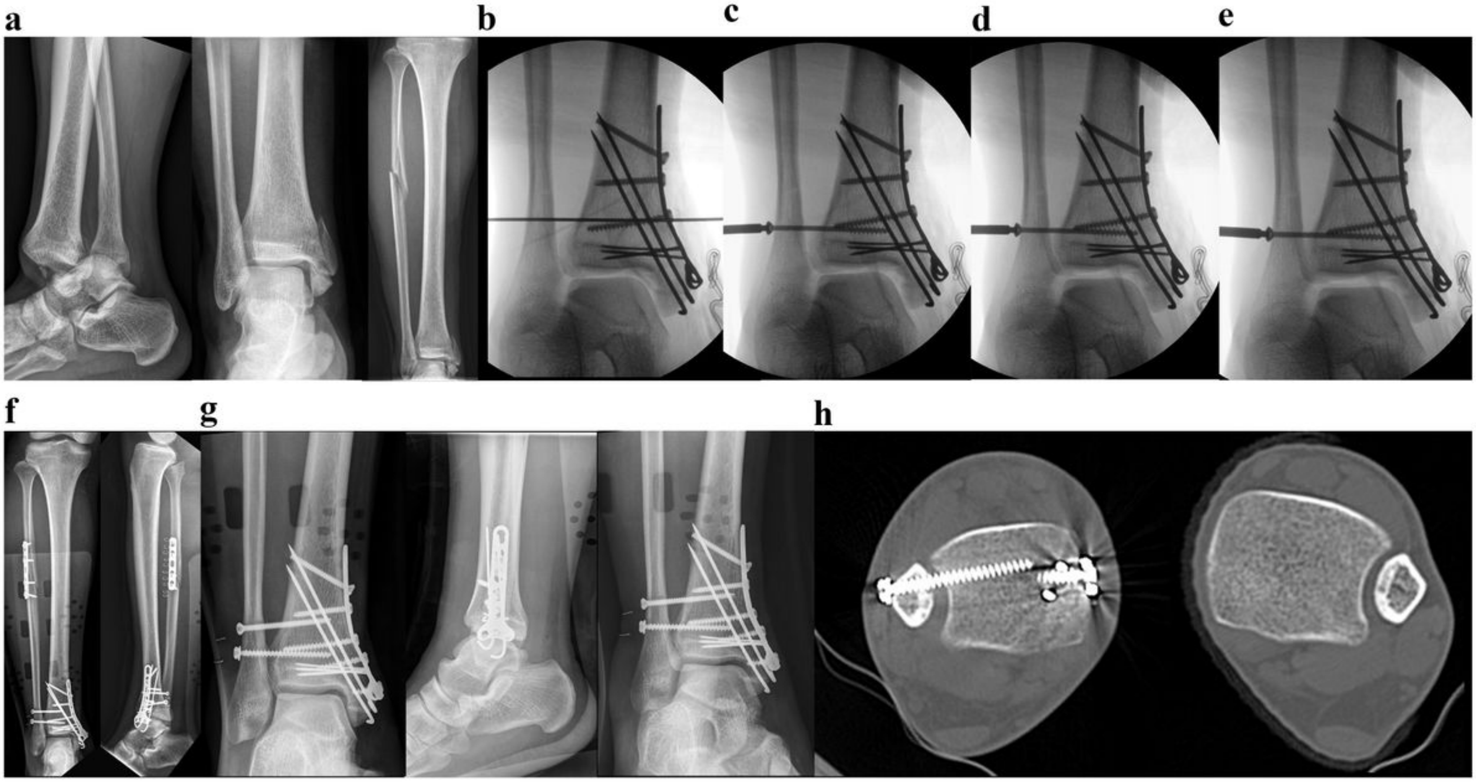

Figure 5

(A) A 36-year-old man sustained an ankle dislocation. (B) After fixing the medial malleolus, the proximal end of the incisura fibularis was localized. (C) The syndesmotic screw was inserted in the expected site based on the tibial tubercle view. (D, E) Compressive force was applied through the cortical screw and showed a positional change in the lateral border of the talus compared to the distal tibia. (F, G) The postoperative radiographs showed good reduction adequacy. (H) The computed tomography images showed that the screw trajectory was directed anteriorly because of excessive internal rotation.

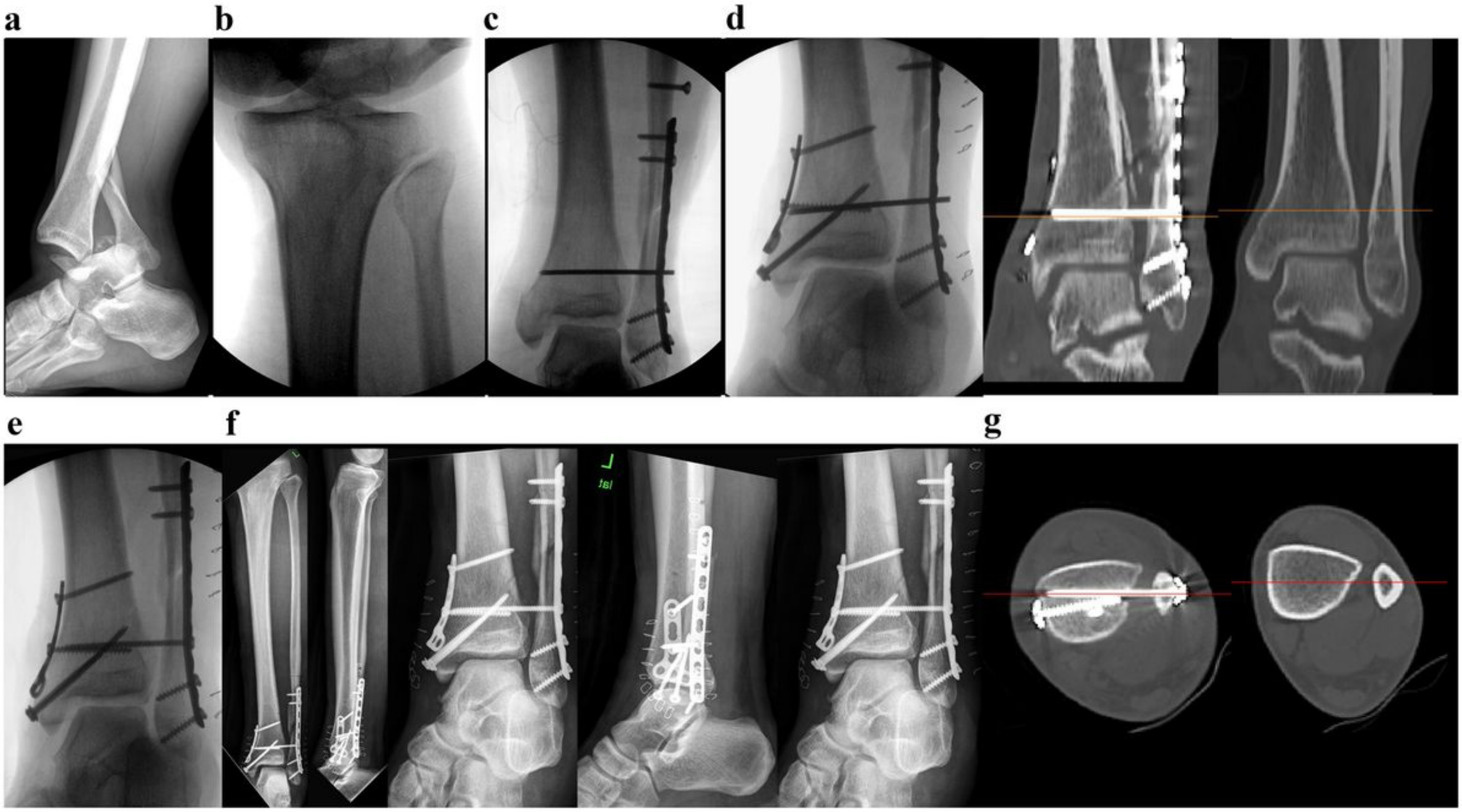

Figure 6

(A) A 53-year-old man sustained an ankle dislocation. (B) After fixing the fibular fracture, the syndesmotic anteroposterior projection was made and (C, D) a K-wire of 2.4 mm was placed as a provisional syndesmotic fixation. (E) After the soft tissue around the ankle settled down, the provisional K-wire was replaced with 3.5 cortical screws. (F) The postoperative radiographs showed good reduction adequacy. (G) The computed tomography images showed that the screw trajectory was the bisecting line of the fibula and incisura.